Wheat Germ Poly(A) Binding Protein Enhances the Binding Affinity of Eukaryotic Initiation Factor 4F and (iso)4F for Cap Analogues†

Chin-Chuan Wei, M. Luisa Balasta, Jianhua Ren, and Dixie J. Goss*

Department of Chemistry of Hunter College of the City University of New York, 695 Park Avenue, New York, New York 10021

Received October 3, 1997; Revised Manuscript Received December 3, 1997

ABSTRACT: Most eukaryotic mRNAs contain a 5′ cap (m^7GpppX) and a 3′ poly(A) tail to increase synergistically the translational efficiency. Recently, the poly(A) binding protein (PABP) and cap-binding protein, eIF-4F, were found to interact [Le et al. (1997) *J. Biol. Chem. 272*, 16247−16255; Tarun and Sachs (1996) *EMBO J. 15*, 7168−7177]. These data suggest that PABP may exert its effect on translational efficiency either by increasing the formation of initiation factor−mRNA complex or by enhancing ribosome recycling. To investigate the functional consequences of these interactions, the fluorescent cap analogue, ant-m^7GTP, which is an environmentally sensitive fluorescent probe [Ren and Goss (1996) *Nucleic Acids Res. 24*, 3629−3634] was used to investigate the cap-binding affinity. Our data show that the binding of eIF-(iso)4F or eIF-4F to cap analogue enhanced their binding affinity toward PABP approximately 40-fold. Similarly, the eIF-4F/PABP or eIF-(iso)4F/PABP complexes show a 40-fold enhancement of cap analogue binding as compared to eIF-4F or eIF-(iso)4F alone. At least part of the enhancement of the translational initiation by PABP can be accounted for by direct changes in cap-binding affinity. The interactions of these components also suggest a mechanism whereby the poly(A) tail is brought into close proximity with m^7G cap. This effect was examined by fluorescence energy transfer, and it was determined that the PABP/eIF-4F complex could bind both poly(A) and 5′ cap simultaneously.

In most eukaryotes, mRNA is required to have both a 5′ cap (m^7GpppX)[1] and a poly(A) tail for efficient translation and message stability (*1*−*6*). These two elements act synergistically to increase translational efficiency, and recent evidence suggests that they communicate during translation (*7*−*9*). The cap serves as the binding site for initiation factors eIF-4F and eIF-(iso)4F, an isozyme form of eIF-4F present in higher plants. The small subunit of eIF-4F (eIF-4E) recognizes the cap structure. eIF-4F interacts with the poly(A) binding protein (PABP) through the 4G subunit, the larger subunit of eIF-4F or eIF-(iso)4F. The cap-associated proteins have a very high binding affinity (nM) for PABP in the absence of poly(A) in the wheat germ system (*9*) but require poly(A) in yeast (*8*). The synergistic effects on translational efficiency may result directly from increased cap affinity of the complex, from efficient recycling of ribosomes, or from a combination of both of these mechanisms. Earlier work (*9*) has shown that PABP interaction with the cap-binding proteins enhanced the affinity for poly(A). This leaves unanswered the question of how interactions at the 3′ end of the mRNA increase translational efficiency. Does PABP also increase the affinity of initiation factors for the cap at the 5′ terminus of mRNA, and if so, is the protein complex of PABP and eIFs capable of binding both the cap and poly(A) simultaneously? Simultaneous binding of both ends of the mRNA is necessary if looping of the mRNA occurs and plays a role in enhancement of translation.

To understand the mechanism of translational enhancement, we have investigated the binary and ternary interactions among the various proteins, m^7G cap analogue, and poly(A) using fluorescence spectroscopy. The data analysis quantitates the interactions of cap-associated proteins and PABP. These quantitative results have allowed us to determine the binding affinity of the cap−protein complex for PABP and the effects of PABP on the cap-binding affinity of eIF-4F and eIF-(iso)4F. PABP increased the cap-binding affinity of both proteins by approximately 40-fold. Furthermore, fluorescence energy transfer experiments demonstrate that the protein complex is capable of binding both cap and poly(A) simultaneously. These results suggest the possibility of RNA looping as a means of translational enhancement and that the synergistic effect of PABP on protein synthesis can be accounted for at least partially by a direct effect on cap affinity of the initiation factors.

EXPERIMENTAL PROCEDURES

Materials. m^7GTP was purchased from Sigma (St. Louis, MO). Nuclease P_1 and poly(A) were purchased from Pharmacia Biotech (Uppsala, Sweden). The synthesis of ant-m^7GTP was carried out as described previously (*10*). The preparation of PABP followed the procedure of Le et al. (*9*) and Yang and Hunt (*11*). The eIF-4F and eIF-(iso)4F were prepared as described elsewhere (*12*, *13*). The concentration of ant-m^7GTP was determined spectrophotometrically using an absorption coefficient of $\epsilon_{332} = 4600\ M^{-1}\ cm^{-1}$. Poly(A)$_{30}$ was prepared by heating 10 mg of poly(A) in the presence of 21 units of Nuclease P_1 at 37 °C, followed by phenol extraction, dialysis, and electrophoresis in 15%

† This work was supported by grants from the National Science Foundation (GER-9023681 and MCB-9722907 to D.J.G).

* To whom correspondence should be addressed. Tel: (212) 772-5383, fax: (212) 772-5332.

[1] Abbreviations: eIF, eukaryotic initiation factor; m^7G, 7-methylguanosine; ant-m^7GTP or cap*, anthraniloyl 7-methylguanosine triphosphate; Tris, tris(hydroxymethyl)aminomethane; DTT, dithiothreitol; EDTA, ethylenediaminetetraacetic acid; BSA, bovine serum albumin; kDa, kilodalton(s).

S0006-2960(97)02457-4 CCC: $15.00
Published on Web 01/30/1998

polyacrylamide gel containing 6.0 M urea and a running buffer containing 0.09 M Tris−borate and 0.002 M EDTA. The gel was examined under UV light. The desired length of poly(A) was compared with oligonucleotide markers. The poly$(A)_{30}$ was cut from the gel, and this gel slice was crushed and eluted with buffer containing 10 mM Tris, pH 8.0, and 0.1 mM EDTA. The 3′-labeling of poly$(A)_{30}$ followed the procedure of Odom et al. (*14*) with some modifications. All reactions were carried out in the dark. Oligonucleotide was oxidized at the 3′ end by incubation with 0.09 M sodium periodate in 0.1 M sodium acetate, pH = 6.0, for 1 h at 37 °C. The reaction was terminated by the addition of KCl. The KIO_4 precipitate was removed by centrifugation at 5000*g* at 4 °C for 10 min. The supernant was dialyzed against 0.1 M sodium acetate, pH 6.0, at 4 °C. The sample was incubated with 1 mM fluorescein thiosemicarbazide at 37 °C for 2 h. At the end of the incubation, the sample was purified by Sephadex G-25 column chromatography. All samples were dialyzed against buffer A (25 mM Tris, 100 mM KOAc, 1 mM $CaCl_2$, 1 mM DDT, 1 mM EDTA, 1 mM $MgCl_2$, pH = 7.6) and passed through a 0.22-μm filter (Millipore, MA) before the spectroscopy measurements were performed. Protein concentrations were estimated by the method of Bradford (*15*) using a Bio-Rad protein assay reagent (Bio-Rad Laboratories, CA).

Spectroscopy Measurements. Absorbance measurements were obtained using a Cary-3 double-beam UV/VIS spectrophotometer. Fluorescence spectra were recorded on a Spex Fluorolog τ_2 spectrofluorometer equipped with excitation and emission polarizers. All measurements were performed at 20 °C. For all equilibrium measurements, at least three titrations were performed, and for fluorescence energy transfer, three reproducible results were obtained. The variation in values for equilibrium constants from different titrations were within 6%.

For measurements of protein−protein interactions, complex formation was studied by monitoring changes in intrinsic protein fluorescence. To maximize the signal, the excitation wavelength was chosen to be 265 nm and emission signal was detected with a cuton filter (50% transmission at 305 nm). Since no emission monochromator was used, the fluorescence intensity change due to fluorescence polarization did not need to be considered. The signal was corrected for light scattering by measuring the buffer under the same conditions. The excitation band-pass was chosen to eliminate photobleaching, and the linearity of fluorescence intensity with protein concentration was determined. For each data point, three samples were prepared. The fluorescence intensity of a solution containing 100 nM PABP was measured. A second sample with a specific amount of cap-binding protein was also measured, and the corrected intensities of the two samples were summed together (F_s). A third sample containing the same amount of PABP and cap-binding protein mixed together was incubated at 20 °C for 20 min, and the corrected fluorescence intensity for this complex was obtained (F_c). The difference in fluorescence intensity related to the complex was defined as $\Delta F = F_c - F_s$. The details of the fitting are described elsewhere (*16*, *17*).

For protein−nucleic acid interactions, the excitation wavelength for ant-m^7GTP was 332 nm and emission was monitored at 420 nm. The excitation slits were chosen to avoid photobleaching, and the absorbance of the sample at the excitation wavelength was less than 0.02 to minimize the inner-filter effect. Emission spectra were corrected for wavelength-dependent lamp intensity and monochromator sensitivities. Steady-state fluorescence anisotropy was measured using an L-format detection configuration. The excitation band-pass was 8.5 nm, and the emission band-pass was 17.0 nm. All samples were incubated at least 15 min at 20 °C before data were collected.

Phase-demodulation lifetime measurements were carried out using a 0.1% (w/w) glycogen suspension in water with a reference lifetime of 0.0 ns. The emission polarizer was placed at a magic angle (54°) to correct for the different sensitivities of the polarized light on the photomultiplier tube and the monochromator.

To determine if energy transfer occurred between the cap-binding analogue and poly(A) when bound to the protein complex, 150 nM ant-m^7GTP, 50 nM eIF-4F, 50 nM PABP, and 50 nM 3′-fluorescein-poly$(A)_{30}$ were mixed together for complex formation with the absorbance at the excitation wavelength of less than 0.02. The fluorescence intensity ($F_{D,A}$) from 380 to 600 nm was recorded. Unlabled m^7GTP and poly$(A)_{30}$ were used as controls since they have almost identical binding affinity as compared with ant-m^7GTP and 3′-fluorescein-poly$(A)_{30}$, respectively. The fluorescence signal from donor (F_D) in the absence of acceptor was determined using 150 nM ant-m^7GTP, 50 nM eIF-4F, 50 nM PABP, and 50 nM poly$(A)_{30}$. The fluorescence signal from acceptor (F_A) at this excitation wavelength was obtained using 150 nM m^7GTP, 50 nM eIF-4F, 50 nM PABP, and 50 nM 3′-fluorescein-poly$(A)_{30}$. Comparison of the spectra obtained from the mixture of both donor and acceptor with the spectra obtained from the sum of individual fluorescence intensities of controls allowed detection of fluorescence energy transfer. The spectral overlap integral, *J*, of the emission spectra of the donor and the absorption spectra of the acceptor was calculated according to

$$J = \frac{\int F_D(\lambda)\epsilon_A(\lambda)\lambda^2 \, d\lambda}{\int F_D(\lambda)\lambda^{-2} \, d\lambda}$$

where $F_D(\lambda)$ is the fluorescence spectrum of the donor and $\epsilon_A(\lambda)$ is the molar absorptivity of the acceptor on a wavelength scale λ. The Förster distance, R_o, between two dyes was not calculated because κ^2, a function of the relative orientation of the dyes, could not be measured directly and the orientation was unlikely to be random.

Data Analysis. The equilibrium constant (K_a) for the binding of ant-m^7GTP with eIFs

$$\text{eIF} + \text{cap*} \Leftrightarrow [\text{cap*}\cdot\text{eIF}]$$

is defined by

$$K_a = \frac{[\text{cap*}\cdot\text{eIF}]}{[\text{cap*}][\text{eIF}]} \quad (1)$$

where [eIF], [cap*], and [cap*·eIF] are the equilibrium concentrations of the unbound protein, ant-m^7GTP, and ant-m^7GTP/protein complex, respectively.

The fluorescence anisotropy, *r*, is defined as

$$r = \frac{I_{VV} - GI_{VH}}{I_{VV} + 2GI_{VH}} \quad (2)$$

where G is a factor that accounts for the polarization bias of the detection system:

$$G = \frac{I_{HV}}{I_{HH}}$$

where I_{HV} and I_{HH} are fluorescence intensity measured with horizontal excitation polarization and with the emission polarizer aligned either vertically or horizontally, respectively.

In a mixture of eIF and ant-m^{7}GTP, the average anisotropy is related to the fraction of the total fluorophore that is bound (f_b) by

$$f_b = \frac{\boldsymbol{r} - \boldsymbol{r}_f}{(\boldsymbol{r}_b - \boldsymbol{r})R + (\boldsymbol{r} - \boldsymbol{r}_f)} \quad (3)$$

where $R = Q_b/Q_f$ is the ratio of quantum yield of the bound and the free ant-m^{7}GTP. $\boldsymbol{r}$, $\boldsymbol{r}_f$, and $\boldsymbol{r}_b$ are the anisotropy values of the mixture, the free ant-m^{7}GTP, and the totally bound ant-m^{7}GTP. It can be shown that the measured anisotropy is related to the total concentration of eIF by

$$r = \frac{a\boldsymbol{r}_b R - a\boldsymbol{r}_f + \boldsymbol{r}_f}{1 + a(R - 1)} \quad (4)$$

where

$$a = (K[\text{cap*}]_T + K[\text{eIF}]_T + 1 - \sqrt{(K[\text{cap*}]_T + K[\text{eIF}]_T + 1)^2 - 4K^2[\text{cap*}]_T[\text{eIF}]_T})/2K[\text{cap*}]_T$$

$[\text{cap*}]_T$, $[\text{eIF}]_T$, and K were the total concentration of ant-m^{7}GTP, protein, and the equilibrium association constant, respectively.

Multifrequency phase and modulation data were analyzed by fitting to a sum of exponentials using the Globals Unlimited program (Urbana, IL).

The measurement of relative quantum yield, Q, of fluorophore was calculated by comparison to a standard whose quantum yield is known (*18*):

$$Q_x = \frac{I_x Q_s A_s}{I_s A_x}$$

where x represents the unknown species, s represents the standard, I is the integrated amount of fluorescence, and A is the absorbance at the excitation wavelength. Disodium fluorescein in 0.01 N NaOH, $Q = 0.92$ (*19*), was used as a standard.

RESULTS

Recently, the binding affinities of cap-associated proteins, eIF-4F, eIF-(iso)4F, and eIF-4B, for PABP were determined (*9*). The data showed the dissociation constants (K_d) were less than 40 nM for eIF-4F and eIF-(iso)4F. For eIF-4B, the K_d was approximately 15 nM. To determine the binding affinities quantitatively, more dilute protein solutions were used. A cuton filter (50% transmission at 305 nm) was used in place of an emission monochromator to monitor the fluorescence signal. The titration curve in Figure 1 shows the difference in fluorescence intensity between the protein−protein complex and the sum of individual fluorescence intensities. The binding curve extrapolates to 1:1 stoichiometry for the two proteins. As a further control, BSA was used to test for nonspecific binding. The fluorescence signal did not show significant change upon addition of BSA (data not shown). The K_d values obtained from data fitting of three curves for the two cap-binding proteins, eIF-4F and eIF-(iso)4F, interacting with PABP are shown in Table 1 (K_2 in Table 1 and Scheme 1). The initiation factor, eIF-4A, which does not bind to the cap region showed no interaction with PABP as reported earlier (*9*).

The fluorescence intensity and maximum emission wavelength of the cap analogue, ant-m^{7}GTP, increased when bound to eIF-4F or eIF-(iso)4F (*10*). The corrected fluorescence spectra for this free cap analogue showed an excitation maximum at 332 nm and emission maximum at 420 nm (*10*). The anisotropy ranged from 0.03 for unbound

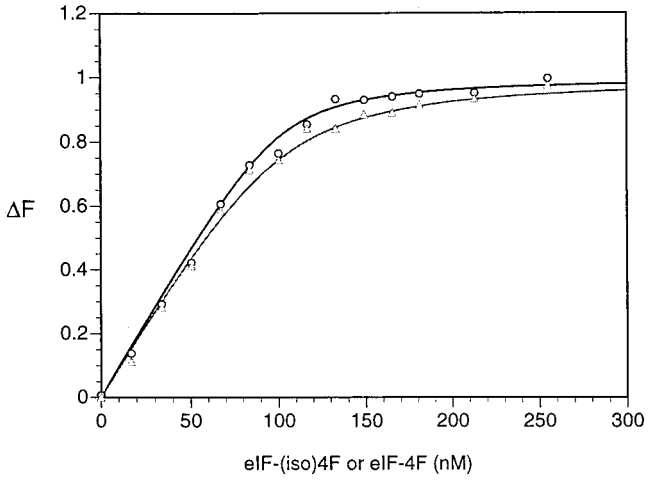

FIGURE 1: Solution of 100 nM PABP was titrated with purified eIF-(iso)4F (circles) and eIF-4F (triangles). The difference between the fluorescence intensities for the combined proteins and the sum of fluorescence intensities of the individual proteins was plotted as a function of the concentration of eIF-(iso)4F or eIF-4F.

Table 1

interactions	K_1[a] (μM)	K_2 (nM)	K_3 (nM)	K_4 (μM)
ant-m^{7}GTP/eIF-(iso)4F/PABP	8.93 ± 1.04	4.3 ± 1.9	0.099 ± 0.045	0.21 ± 0.09
ant-m^{7}GTP/eIF-4F/PABP	4.69 ± 0.33	9.1 ± 4.1	0.23 ± 0.05	0.12 ± 0.06

[a] K represents the dissociation constant. See Scheme 1 for detail of interactions.

Scheme 1

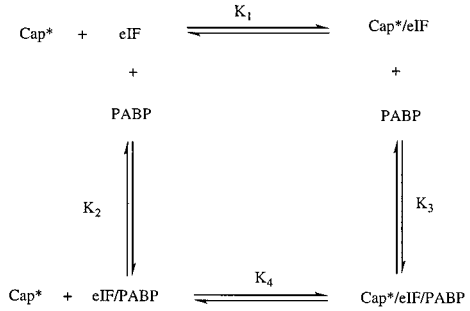

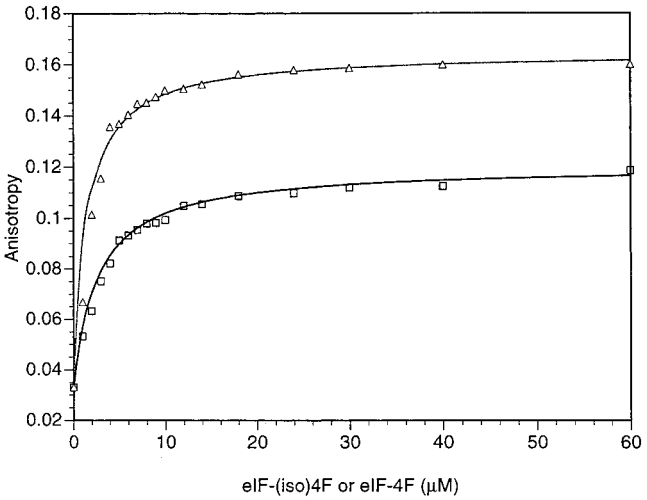

FIGURE 2: Titration of ant-m^{7}GTP with eIF-4F (triangles) and eIF-(iso)4F (squares). Titrations were performed in buffer A. Concentration of ant-m^{7}GTP was 0.3 μM. Complex formation was monitored by steady-state anisotropy. The solid line presents the best fit of the data to eq 4.

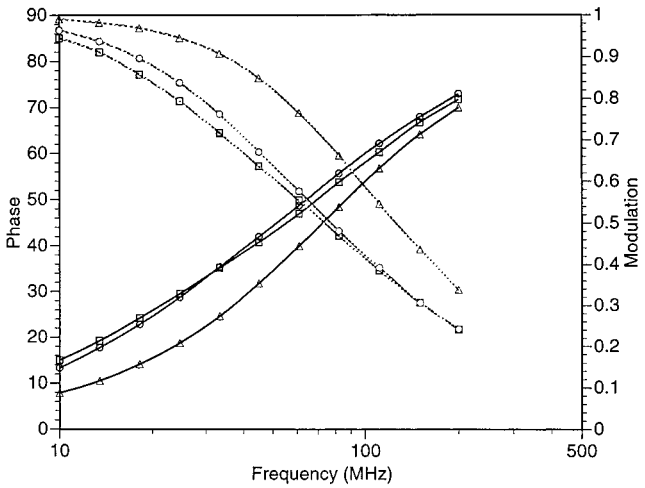

FIGURE 3: Phase and modulation values as a function of frequency for ant-m^{7}GTP bound to eIF-(iso)4F. ant-m^{7}GTP alone (triangles): The solid line was fitted as a one-exponential decay with a lifetime of 2.0 ns. ant-m^{7}GTP and eIF-(iso)4F (squares): The solid line corresponds to a two-exponential component fit of the data with lifetimes $\tau_1 = 1.98$ ns and $\tau_2 = 6.93$ ns having a fractional amplitude $f_1 = 0.513$ and $f_2 = 0.487$. ant-m^{7}GTP and eIF-4F (circles): The solid line represents $\tau_1 = 2.01$ ns and $\tau_2 = 5.04$ ns having a fraction amplitude $f_1 = 0.404$ and $f_2 = 0.596$.

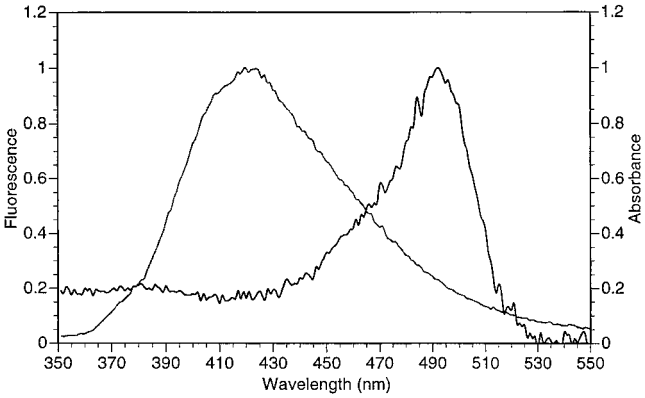

FIGURE 4: Spectral overlap of absorption spectrum (thick line) of 3′-fluorescein-poly(A)$_{30}$ and emission spectrum (thin line) of ant-m^{7}GTP in the buffer A. For presentation, absorbance and fluorescence were normalized to have the same maximum values.

fluorophore to 0.12 for ant-m^{7}GTP/eIF-(iso)4F (Figure 2). The ant-m^{7}GTP/eIF-4F complex had an anisotropy value of 0.16. By fitting the data according to eq 4, the K_d values (K_1 in Table 1 and Scheme 1) were calculated to be 8.93 $\pm$ 1.04 μM for ant-m^{7}GTP/eIF-(iso)4F and 4.69 $\pm$ 0.07 μM for ant-m^{7}GTP/eIF-4F (Figure 2). These data are similar to those obtained for m^{7}G$_{ppp}$G binding (*20*), which is consistent with the fact that most nucleotide-binding proteins are sensitive to structural variations in the purine ring, but modifications of the ribose moiety have little effect on binding affinity (*21*−*23*). The characteristic anisotropy of the ant-m^{7}GTP/eIF-4F complex was higher than that of the ant-m^{7}GTP/eIF-(iso)4F complex because the eIF-4F has the almost twice the molecular weight of eIF-(iso)4F (246 kDa as compared to 114 kDa) while the fluorescence lifetimes of the complexes were similar. The observed steady-state anisotropy depends on the correlation time (t_c) of the fluorophore and its lifetime (*24*). Free ant-m^{7}GTP has a fluorescence excited-state lifetime of 2.0 ns (Figure 3). Lifetime measurements on the ant-m^{7}GTP/eIF-(iso)4F showed a longer lifetime of 6.8 ns attributable to the protein complex. The ant-m^{7}GTP/eIF-4F complex has a shorter lifetime of 5.0 ns. The fluorescence enhancement and longer lifetime of the protein-bound form of ant-m^{7}GTP may be due to the formation of hydrogen bond(s), which stabilize its charge-transfer excited state, or the cap-binding pocket may be a more hydrophobic region (*25*). The recent X-ray crystal structure of murine eIF-4E (*26*) indicates that 7-methyl G recognition is mediated by the guanosine base interaction between two conserved tryptophans plus formation of three hydrogen bonds and a van der Waals interaction between its N-7 methyl group and a third conserved tryptophan. The ribose of the cap is located in a hydrophobic region, which may allow the nonprotonated chromophore of the ant-m^7-GTP to enter the binding pocket. Stabilization of the polar excited state would result in a longer lifetime.

It has been previously reported (*7*) that eIF-(iso)4F, eIF-4F, and eIF-4B bound to the mRNA poly(A) tail. The size of the binding sites of eIF-4F and eIF-4B were estimated to be 25 bases in a buffer containing 150 mM KCl (*27*). From the packing density measurement, PABP was also found to bind 25 A residues per molecule (*28*). To determine whether the cap and poly(A) tail were bound to separate sites on this protein complex, energy transfer experiments were performed. The fluorescence probe, fluorescein, was attached to the 3′ end of poly(A)$_{30}$. The spectral overlap between fluorescence emission of ant-m^{7}GTP and absorbance of fluorescein labeled poly(A) (Figure 4) allowed fluorescence energy transfer to be monitored. Titration of 3′-fluorescein-poly(A)$_{30}$ with eIF-4F and PABP showed no significant fluorescence intensity changes, but an anisotropy change was observed indicating formation of a nucleic acid−protein complex. As a control, m^{7}GTP and unlabeled poly(A)$_{30}$ were used. Figure 5 shows the spectrum obtained from the complex, ant-m^{7}GTP/eIF-4F/PABP/3′-fluorescein-poly(A)$_{30}$ and the spectrum from the sum of the spectra for m^{7}GTP/eIF-4F/PABP/3′-fluorescein-poly(A)$_{30}$ and ant-m^{7}GTP/eIF-4F/PABP/poly(A)$_{30}$. Essentially the same results were obtained with three different experiments using two different PABP preparations. The fluorescence quenching at 420 nm and enhancement at 510 nm demonstrated that eIF-4F/PABP

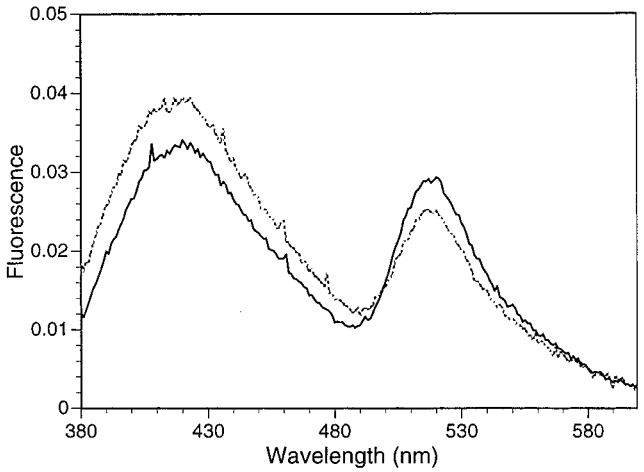

FIGURE 5: Fluorescence energy transfer. The solid line is the measured fluorescence intensity of ant-m^{7}GTP/eIF-4F/PABP/3′-fluorescein-poly(A)$_{30}$. The broken line is the sum of the fluorescence spectra for m^{7}GTP/eIF-4F/PABP/3′-fluorescein-poly(A)$_{30}$ and ant-m^{7}GTP/eIF-4F/PABP/poly(A)$_{30}$. The increase in acceptor fluorescence at 510 nm and corresponding decrease in fluorescence at 420 nm indicates energy transfer between the cap and poly(A) tail. The concentration used for ant-m^{7}GTP (m^{7}GTP), eIF-4F, PABP, and 3′-fluorescein-poly(A)$_{30}$ (poly(A)$_{30}$) were 150, 50, 50, and 50 nM, respectively.

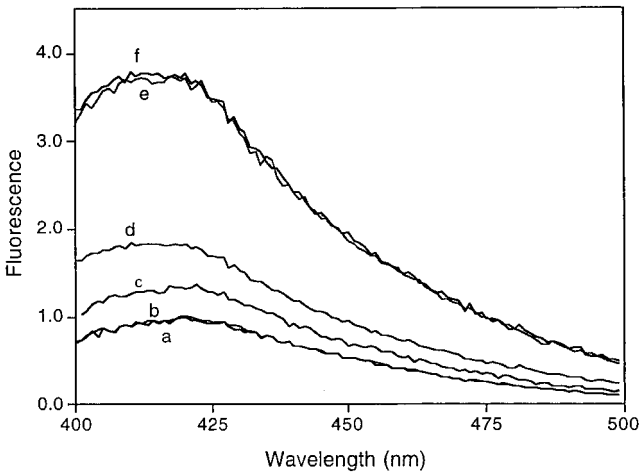

FIGURE 6: Corrected fluorescence emission spectra of 25 nM ant-m^{7}GTP (pH 7.5) (a) ant-m^{7}GTP alone, (b) +0.4 μM PABP, (c) +0.02 μM eIF-(iso)4F, (d) +0.02 μM eIF-(iso)4F and 0.01 μM PABP, (e) +1.5 μM eIF-(iso)4F, and (f) +1.5 μM eIF-(iso)4F and 25 μM PABP. All samples were excited at 332 nm.

bound both fluorescent cap analogue and fluorescent poly(A) simultaneously. At these concentrations, the two proteins will be present almost entirely as a complex. The cap analogue, however, will have some fluorophore unbound. This may partially explain the efficiency of the energy transfer.

For ternary ant-m^{7}GTP/eIF-(iso)4F/PABP and ant-m^{7}GTP/eIF-4F/PABP studies, steady-state fluorescence spectra were examined. Figure 6 shows the emission spectra of different ant-m^{7}GTP complexes excited at 332 nm. The ant-m^{7}GTP, when excited at 332 nm, shows a maximum fluorescence intensity at 420 nm. Upon addition of PABP, no fluorescence intensity change was observed, indicating that no interaction between this cap analogue and PABP occurred. This result was confirmed using anisotropy and lifetime measurements (data not shown), which also do not show any change upon addition of PABP. Fluorescence intensity was enhanced and the emission wavelength maximum shifted when eIF-(iso)4F was added to the cap analogue. Under conditions where concentrations of eIF-(iso)4F and PABP are larger than the concentration of cap analogue, no significant fluorescence intensity difference between cap analog/eIF complex and cap analog/eIFs/PABP complex was observed. The lifetime analysis on this ternary system could be fitted as two-exponential decay with the same results as ant-m^{7}GTP/eIF-(iso)4F system (one short lifetime for ant-m^{7}GTP and a longer lifetime for the protein complex). Similar results were obtained for the cap analog/eIF-4F/PABP complex. This suggested that the microenvironment of the cap analogue was similar in the cap analog/eIF and the cap analog/eIF/PABP complexes.

A typical binding isotherm can be developed as described elsewhere (*29*). For a simple binary reaction:

$$\text{cap}^* + \text{eIF} \Leftrightarrow \text{cap}^*\cdot\text{eIF}$$

$$F = \frac{KF_1[\text{eIF}] + F_0}{1 + K[\text{eIF}]} \tag{5}$$

$$[\text{eIF}] = (-(1 + K[\text{cap}^*]_T - K[\text{eIF}]_T) + \sqrt{(1 + K[\text{cap}^*]_T - K[\text{eIF}]_T)^2 + 4K[\text{eIF}]_T})/2K$$

Equation 5 can be solved for association constant (K) and where cap*, eIF, and cap*·eIF are free fluorescent ant-m^7-GTP, cap-binding protein, and ant-m^{7}GTP/eIF complex, respectively. $[\text{cap}^*]_T$ and $[\text{eIF}]_T$ are the total concentrations of ant-m^{7}GTP and protein, respectively. F is the measured value of the fluorescence intensity at any point in the titration; F_0 and F_1 are the fluorescence intensities at the start and at the end of the titration. Thus, K can be obtained by fitting the experimental data using nonlinear regression analysis. In principle, any one point will give a K value if the initial and final points are known, there is therefore considerable redundancy in the data fitting.

For the ternary system, the fluorescence data were treated analogously. Binding of eIFs to PABP in the presence of cap analogue can be described as shown in Scheme 1. From our previous data, PABP does not bind to the cap analogue under these conditions. K_1 and K_2 are dissociation constants for ant-m^{7}GTP/eIF and eIF/PABP, respectively. K_3 and K_4 are dissociation constants for cap analogue/eIFs to PABP and eIFs/PABP to cap analogue, respectively. Thermodynamically, $K_1K_3 = K_2K_4$. In accordance with Scheme 1, the apparent association constant (K_{app}) is derived as follows:

$$K_{app} = \frac{([\text{cap}^*\cdot\text{eIF}]) + (F_2/F_3)[\text{cap}^*\cdot\text{eIF}\cdot\text{PABP}]}{[\text{cap}^*]([\text{eIF}] + [\text{eIF}\cdot\text{PABP}])}$$

$$= \frac{\dfrac{([\text{cap}^*\cdot\text{eIF}]) + (F_2/F_3)[\text{cap}^*\cdot\text{eIF}\cdot\text{PABP}]}{[\text{cap}^*][\text{eIF}]}}{\dfrac{[\text{cap}^*]([\text{eIF}] + [\text{eIF}\cdot\text{PABP}])}{[\text{cap}^*][\text{eIF}]}}$$

$$= \frac{(1/K_1) + (F_2/F_3)(1/K_1)(1/K_3)[\text{PABP}]}{1 + (1/K_2)[\text{PABP}]} \tag{6}$$

where [PABP] was the concentration of free PABP and F_2

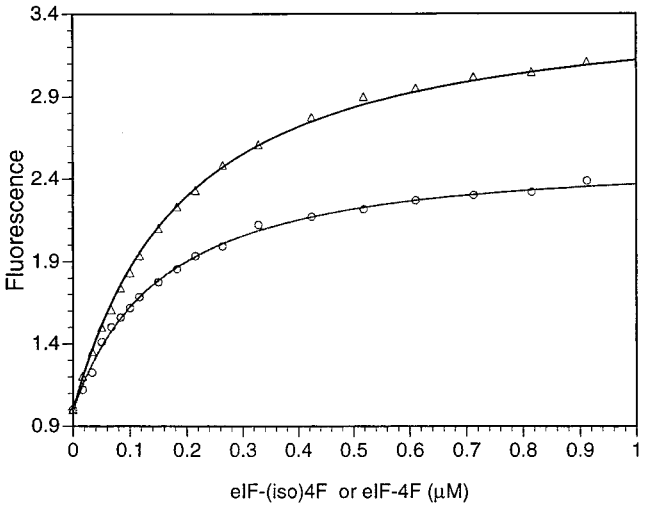

FIGURE 7: Binding of eIF-(iso)4F (triangles) or eIF-4F (circles) to PABP and ant-m^{7}GTP. Concentrations of ant-m^{7}GTP and PABP were 25 nM and 20 μM, respectively. The solid line represents the best fit to eq 5. Excitation was at 332 nm, and fluorescence emission was integrated from 400 to 500 nm.

and F_3 are fluorescence intensities (integrated from 400 to 500 nm) of ant-m^{7}GTP/eIF and ant-m^{7}GTP/eIF/PABP complexes, respectively. Under conditions where [PABP] $\gg$ [cap*] and [PABP] $\gg$ [eIFs], [PABP] = $[PABP]_T$, where $[PABP]_T$ was the total concentration of PABP. This equation has only one variable, K_3 or K_4. Titration curves where 25 nM ant-m^{7}GTP and 20 μM PABP were titrated with eIF-(iso)4F or eIF-4F are shown in Figure 7. The solid line represents the best fit of the data for eq 5. The K_{app} value obtained was $(5.02 \pm 0.12) \times 10^6$ M^{-1} and $(8.13 \pm 0.24) \times 10^6$ M^{-1} for ternary cap ant-m^{7}GTP/eIF-(iso)4F/PABP and ant-m^{7}GTP/eIF-4F/PABP system, respectively. Theoretically, from eq 6, K_{app} is a function of [PABP]. By changing the concentration of PABP, we could solve for all of the K_d values in Scheme 1 by nonlinear regression analysis without individual binding measurements. However, limitations on the amount of protein needed made this impractical. The fitted values of K_3 for PABP dissociation from ant-m^{7}GTP/eIF/PABP complexes were in the nanomolar range, while values of K_4 for ant-m^{7}GTP dissociation from the ant-m^7-GTP/eIF/PABP complexes were in the micromolar range. Increasing the concentration of PABP 2-fold did not alter K_{app} significantly (data not shown). This result was reasonable considering the K_1 and K_2 values obtained from separate titrations since any concentration of PABP used in the micromolar range will be canceled out in eq 6. The exact values of K_d for eIF-(iso)4F and eIF-4F are summarized in Table 1. The presence of cap analogue enhances the binding eIF to PABP approximately 40-fold. The binding affinities of the eIF/PABP complexes to cap analogue were enhanced approximately 40-fold as compared to the affinity of cap-binding proteins alone. The two cap-binding proteins, eIF-4F and eIF-(iso)4F behaved very similarly. In both cases, the presence of PABP enhanced cap-binding affinity and the presence of the cap-enhanced protein complex formation.

DISCUSSION

PABP has known RNA binding motifs, but here we have demonstrated protein−protein interactions as well as the effects of these interactions on cap-binding affinity. PABP has been shown to influence translation, but the mechanism is unclear. Direct fluorescence titrations demonstrated that the interaction of PABP with eIF-4F and eIF-(iso)4F increase the cap binding affinity by an order of magnitude.

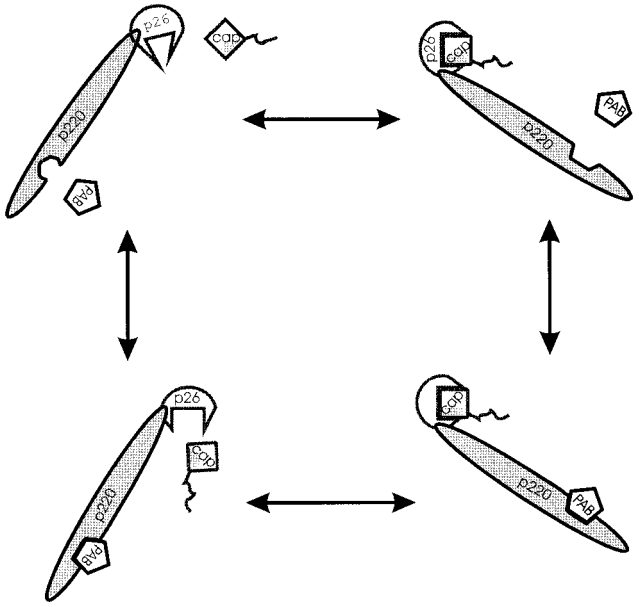

FIGURE 8: Schematic diagram for the interaction of ant-m^{7}GTP, eIF-4F, and PABP. The eIF-4F is presented as two subunits, eIF-4G and eIF-4E.

Fluorescence energy transfer studies on these cap-binding proteins/PABP complex indicate that they have different binding sites for the 5′ cap and 3′ poly(A) tail. Even though cap analogue binds to eIF-4F or eIF-(iso)4F with a K_d of 4−9 μM, in the presence of PABP, cap binding is enhanced 40-fold. Similarly, cap bound to cap-binding protein will enhance the binding to PABP. Since cap analogues have been demonstrated by CD analysis to induce a conformational change in eIF-(iso)4F (*30*), this may explain the higher affinity of cap-eIF for PABP. The data presented here support a model where eIF-4F, PABP, and cap are involved in formation of an RNA complex, which is summarized in Figure 8. The model shows the microenvironment of the cap to be similar in the ant-m^{7}GTP/eIF-4F and ant-m^{7}GTP/eIF-4F/PABP complexes, since no significant change in fluorescence intensity or lifetime measurements occurred. The binding of cap to eIF-4F results in conformational changes in eIF-4F, which subsequently enhance the binding to PABP. eIF-4F bound to PABP may have a conformation change in order to bring the nonpolar domains together, which would subsequently enhance cap binding.

The fact that PABP enhances the affinity of eIF-4F or eIF-(iso)4F for the cap analogue is an interesting observation in light of fact that PABP interacts with the 4G subunit (*8, 9*) and not directly with the cap-binding subunit, 4E. These results suggest that a conformational change is propagated through the 4G subunit to the cap binding subunit, 4E. Enhancement of translation by PABP may be at least partially accounted for by a direct effect on the cap affinity. Additional enhancement may occur through a mechanism whereby the 5′ and 3′ ends of mRNA interact and ribosomes are more readily recycled.

REFERENCES

1. Jackson, R. J., and Standart, N. (1990) *Cell 62*, 15−24.
2. Munroe, D., and Jacobson A. (1990) *Mol. Cell. Biol. 10*, 3441−3455.
3. Munroe, D., and Jacobson A. (1990) *Gene 91*, 151−158.
4. Bernstein, P., and Ross, J. (1989) *Trends Biochem. Sci. 14*, 373−377.
5. Sonenberg, N. (1988) *Prog. Nucleic Acid Res. Mol. Biol. 35*, 173−207.
6. Rhoads, R. E. (1988) *Trends Biochem. Sci. 13*, 52−56.
7. Gallie, D. R., and Tanguay, R. L. (1994) *J. Biol. Chem. 269*, 17166−17173.
8. Tarun, S. Z., Jr., and Sachs, A. B. (1996) *EMBO J. 15*, 7168−7177.
9. Le, H., Tanguay, R. L., Balasta, M. L., Wei, C.-C., Browning, K. S., Goss, D. J., and Gallie, D. R. (1997) *J. Biol. Chem. 272*, 16247−16255.
10. Ren, J., and Goss, D. J. (l996) *Nucleic Acids Res. 24*, 3629−3634.
11. Yang, J., and Hunt, A. G. (1992) *Plant Physiol. 98*, 1115−1120.
12. Lax, S. R., Lauer, S. J., Browning, K. S., and Ravel, J. M. (1986) *Methods Enzymol. 118*, 109−128.
13. Lax, S. R., Browning, K. S., Maia, D. M., and Ravel, J. M. (1986) *J. Biol. Chem. 261*, 15632−15636.
14. Odom, O. W., Jr., Robbins, D. J., Lynch, J., Dottavio-Martin, D., Kramer, G., and Hardesty, B. (1980) *Biochemistry 19*, 5947−5954.
15. Bradford, M. M. (1976) *Anal. Biochem. 72*, 248−254.
16. Firpo, M. A., Connelly, M. B., Goss, D. J., and Dahlberg, A. E. (1996) *J. Biol. Chem. 271*, 4693−4698.
17. Locke, B. C., MacInnis, J. M., Qian, S.-J., Gordon, J. I., Li, E., Fleming, G. R., and Yang, N.-C. (1992) *Biochemistry 31*, 2376−2383.
18. Freifelder, D. (1976) *Physical Biochemistry: Applications to Biochemistry and Molecular Biology*, pp 440−441, W. H. Freeman, San Francisco.
19. Weber, G., and Teale, F. W. J. (1957) *Trans. Faraday Soc. 53*, 646−655.
20. Goss, D. J., Carberry, S. E., Dever, T. E., Merrick, W. C., and Rhoads, R. E. (1990) *Biochim. Biophys. Acta 1050*, 163−166.
21. Darzynkiewicz, E., Stepinski. J., Ekiel, I., Goyer, C., Sonenberg, N., Temeriusz, A., Jin, Y., Sijuwade, T., Haber, D., and Tahara, S. M. (1989) *Biochemistry 28*, 4771−4778.
22. Darzynkiewicz, E., Stepinski, J., Ekiel, I., Jin, Y., Haber, D., Sijuwade, T., and Tahara, S. M. (1988) *Nucleic Acids Res. 16*, 8953−8962.
23. Darzynkiewicz, E., Ekiel, I., Lassota, P., and Tahara, S. M. (1987) *Biochemistry 26*, 4372- 4380.
24. Lakowicz, J. R. (1983) *Principles in Fluoresence Spectroscopy*, Plenum Press, New York.
25. Birmachu, W., and Reed, J. K. (1988) *Photochem. Photobiol. 47*, 675−683.
26. Marcotrigiano, J., Gingras, A.-C., Sonenberg, N., and Burley, S. K. (1997) *Cell 89*, 951−961.
27. Goss, D. J., Woodley, C. L., and Wahba, A. J. (1987) *Biochemistry 26*, 1551−1556.
28. Sachs, A. B., Davis, R. W., and Kornberg, R. D. (1987) *Mol. Cell. Biol. 7*, 3268−3276.
29. Heyduk, T., and Lee, J. C. (1990) *Proc. Natl. Acad. Sci. U.S.A. 87*, 1744−1748.
30. Wang, Y., Sha, M., Ren, W. Y., van Heerden, A., Browning, K. S., and Goss, D. J. (1996) *Biochim. Biophys. Acta 1297*, 207−213.

BI9724570